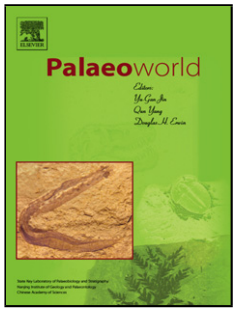

Title: Miocene mammalian faunas from Wushan, China and their evolutionary, biochronological, and biogeographic significances

Authors: Bo-Yang Sun, Xiu-Xi Wang, Min-Xiao Ji, Li-Bo Pang, Qin-Qin Shi, Su-Kuan Hou, Dan-Hui Sun, Shi-Qi Wang

PII: S1871-174X(17)30054-9
DOI: http://dx.doi.org/10.1016/j.palwor.2017.08.001
Reference: PALWOR 427

To appear in: *Palaeoworld*

Received date: 23-4-2017
Revised date: 31-7-2017
Accepted date: 22-8-2017

Please cite this article as: Sun, Bo-Yang, Wang, Xiu-Xi, Ji, Min-Xiao, Pang, Li-Bo, Shi, Qin-Qin, Hou, Su-Kuan, Sun, Dan-Hui, Wang, Shi-Qi, Miocene mammalian faunas from Wushan, China and their evolutionary, biochronological, and biogeographic significances.Palaeoworld http://dx.doi.org/10.1016/j.palwor.2017.08.001

Miocene mammalian faunas from Wushan, China and their evolutionary, biochronological, and biogeographic significances

Bo-Yang Sun [a, b, c], Xiu-Xi Wang [d], Min-Xiao Ji [d], Li-Bo Pang [e], Qin-Qin Shi [a], Su-Kuan Hou [a], Dan-Hui Sun [a, b], Shi-Qi Wang [a, f] *

[a] Key Laboratory of Vertebrate Evolution and Human Origins of Chinese Academy of Sciences, Institute of Vertebrate Paleontology and Paleoanthropology, Chinese Academy of Sciences, Beijing 100044, China

[b] University of Chinese Academy of Sciences, Beijing 100039, China

[c] Laboratory of Evolutionary Biology, Department of Anatomy, College of Medicine, Howard University, Washington D.C. 20059, USA

[d] Key Laboratory of Western China's Environmental Systems (Ministry of Education), College of Earth and Environmental Sciences, Lanzhou University, Lanzhou 730000, China

[e] China Three Gorges Museum, Chongqing 400013, China

[f] CAS Center for Excellence in Tibetan Plateau Earth Sciences, Beijing 100101, China

* Corresponding author. *E-mail address*: wangshiqi@ivpp.ac.cn

Abstract

We report Miocene mammalian faunas from three nearby localities: Kangping, Nanyu, and Yangping, in the Wushan Subbasin, Gansu Province, China. From the Kangping locality, we identified four species, *Platybelodon grangeri*, *Hispanotherium wushanense* n. sp., *Kubanochoerus* sp., and *Turcocerus* cf. *kekemaidengensis*, which indicate that this fauna can be correlated with MN7/8. From the Nanyu locality, we identified *Platybelodon* aff. *tongxinensis*, which, together with the previously reported specimens of *Gomphotherium wimani* and *Micromeryx* cf. *flourensianus*, enables us to correlate this fauna with MN6. The Yangping locality is found to be early Miocene in age based on the presence of cf. *Gomphotherium* sp. This occurrence is the earliest

record of proboscideans in China, and thus represents the "Proboscidean Datum Event". Evolutionary trends of *Platybelodon* and *Hispanotherium* are figured and discussed. The possibility of a geographic boundary associated with the eastern and western differentiation of species of *Turcocerus* and bunodont listriodonts in China is also evaluated. This boundary was consistent with the major division of the eastern and western mammalian faunas of the middle Miocene in China. The localities in Inner Mongolia suggest a large area with transitional habitats.

Keywords: Wushan Subbasin; Miocene; fauna; age; evolution; paleozoogeography

1. Introduction

In the middle Miocene of China, the environment was entering a transitional period, and the mammalian fauna was rapidly diversifying (Qiu and Qiu, 1995; Zachos et al., 2001; Zhang and Guo, 2005; Deng, 2011). Systematic research on the middle Miocene mammalian faunas of China began with the Central Asiatic Expedition organized by the American Museum of Natural History in 1928, when the first ‘‘Pliocene’’ locality was found near a freshwater well locally known as Gur Tung Khara Usu in central Inner Mongolia (Spock, 1929; Andrews, 1932; Wang et al., 2003). The middle Miocene in particular, which is divided into an early interval (MN6, 15–13.5 Ma) and a late interval (MN7/8, 13.5–11.1 Ma), has attracted a great deal of attention in China (Deng et al., 2013) because of the richness and excellent preservation of the findings. Consequently, many middle Miocene fossil assemblages have been found in China. Ten mammalian faunas of MN6 have been reported: the Tairum Nor (Wang et al., 2003; Deng et al., 2007), Dingjiaergou (Qiu and Qiu, 1995; Wang et al., 2016b), Jiulongkou (Chen and Wu, 1976), Lengshuigou (Qiu and Qiu, 1990), Erlanggang (Yan, 1979), Shinanu, Zengjia (Guan, 1988; Cao et al., 1990; Deng et al., 2013; Wang, 2014), Lierpu (Li et al., 1981; Qiu et al., 1981; Deng, 2004b), Quantougou (Qiu, 2000, 2001a, 2001b; Qiu and Li, 2003; Deng et al., 2007), and Halamagai (Wu et al., 1998, 2003; Ye et al., 2001) faunas. In addition, seven mammalian faunas of MN7/8 have been reported: the Moergen (Qiu et al., 2006, 2013;

Deng et al., 2007), Laogou (Deng, 2003, 2004a; Deng et al., 2013), Olongbuluk (Wang et al., 2007), Damiao (Zhang et al., 2011), Koujiacun (Liu et al., 1960), Kekemaideng (Ye, 1989; Ye et al., 1999, 2001) and Xiaolongtan (Dong, 1987) faunas. New middle Miocene fossil assemblages are needed for spatiotemporal comparison, and are likely to be discovered in locations where thick Miocene basin fills were deposited and thereafter incised, such as in central Gansu Province, China.

2. Geological setting

The Wushan Subbasin is located in the west of the Tianshui Basin (Fig. 1). Wang et al. (2013b, 2015) reported mammalian fossils from the Nanyu locality, and identified these fossils as *Gomphotherium wimani* and *Micromeryx* cf. *flourensianus*, which are middle Miocene in age. Recently, new material was collected from the same area, including the previously reported Nanyu locality, and two newly discovered localities at Kangping and Yangping. These three localities show a clear superposition relationship (Kangping, Nanyu, and Yangping, from uppermost to lowermost) based on stratigraphic correlation (Fig. 2).

3. Material and methods

Specimens we report in this research were from three localities, Yangping, Nanyu and Kangping. Most of them were collected from Kangping which is correlated with MN7/8. The Nanyu locality, as we have shown, is correlated with MN6, and the Yangping locality is correlated with the early Miocene based on the presence of a very primitive gomphothere, although the specimens are fragmentary.

The terminology of maxilla and mandible structures follows Sisson (1953); that of occlusal structures of teeth for proboscideans, rhinocerotids, suids, and bovids follows Tassy (2014), Qiu and Wang (2007), van der Made (1996), and Gentry (1992), respectively.

Abbreviations: CEESV: Key Laboratory of Western China's Environmental Systems (Ministry of Education), College of Earth and Environmental Sciences, vertebrate collection, Lanzhou University, Lanzhou, China; IVPP V: Institute of

Vertebrate Paleontology and Paleoanthropology, vertebrate collection, Beijing, China; HMV: Hezheng Paleozoological Museum, vertebrate collection, Hezheng, China.

4. Systematic paleontology

Class MAMMALIA Linnaeus

Order PROBOSCIDEA Illiger

Family GOMPHOTHERIIDEA Hay

Genus indet. cf. *Gomphotherium* Bermeister

cf. *Gomphotherium* sp.

(Fig. 3A, B)

Locality: Yangping.

Referred specimen: CEESV0034, molar fragment.

Description and comparison: CEESV0034 is a fragment of a proboscidean molar (Fig. 3A, B), as indicated by the conical enamel pillars. We can approximately identify the pretrite conelet, the mesoconelet, and central conules of a certain loph(id). The occurrence of a proboscidean indicates the age of the Yangping locality: the Shanwangian of the early Miocene.

Family AMEBELODONTIDAE Barbour

Genus *Platybelodon* Borissiak

Platybelodon aff. *tongxinensis* Chen

(Fig. 3C, F, G)

Holotype: IVPP V5572, a pair of M3 and m3 of the same individual.

Locality: Nanyu.

Geographic distribution: Tongxin, Ningxia; Citan, Gansu; Wushan, Gansu; all in

China.

Stratigraphic distribution: middle Miocene, MN6.

Referred specimens: CEESV0025, right m3; CEESV0026, right humerus.

Description: The m3 (Fig. 3C) is barely erupted from the first lophid, and the posterior lophids were exposed by removing the bony cover of the mandibular fragment. The specimen is composed of four lophids and a distal enamel conelet that rises from the posterior cingulid. The first pretrite half-lophid is broken. The pretrite half-lophids are marked by well-developed trefoils on the first three lophids, the mesoconelets of which are shifted anteriorly to merge with the anterior accessory central conules, whereas the strong, serrated and individualized posterior accessory central conules tend to invade the neighboring entoflexid. The corresponding posttrite half-lophids have mesoconelets and anterior accessory central conules. On the posterior lophids, the mesoconelets and anterior accessory central conules of the pretrite, and posttrite half-lophids are either separated or fused, but tend to reduce from anterior to posterior or are entirely absent. The pretrite and posttrite sides of the same lophid show alternating positions. The posterior cingulid is composed of one or two large conelets, and the cingulid is also developed on the anterior border of the tooth. The cementum in the interlophs is strong. The small conules in the interlophids are weakly developed.

The humerus (Fig. 3F, G) is damaged, and lacks the lateral tuberosity and parts near the proximal and distal sides and the lateral condyle. The proximal end is robust, and the head is large and rounded. The deltoid tuberosity is strong and thick. The whole bone tapers rapidly from proximal to distal. The internal surface of the medial condyle is rough.

Comparison: The narrow contour, subhypsodonty, strong chevron of the half-lophids, and serrated posterior central conules that invade the neighboring entoflexid support attribution of the tooth to *Platybelodon*. Although the tooth is still a germ, it has only four lophids, which can be distinguished from the five-lophid m3 of *Platybelodon grangeri*. Here we refer to this specimen as *P.* aff. *tongxingensis*, which generally has four-lophid m3. Although *Gomphotherium wimani* has been reported from the same

locality, we identify the proboscidean humerus as *P. tongxingensis* because of its slenderness (Fig. 4, Table 1), which appears to be a character of the limbs of *Platybelodon* (Wang and Ye, 2015).

Platybelodon grangeri Osborn

(Fig. 3D, E)

Locality: Kangping.

Geographic distribution: Laogou and Zengjia, Linxia, Gansu; Tunggur, Inner Mongolia; Halamagai, Xinjiang; Zhongning, Ningxia; Wushan, Gansu; all in China.

Stratigraphic distribution: late middle Miocene, MN7/8.

Referred specimens: CEESV0024, right DP4; CEESV0037, left mandibular fragment with broken dp3 and dp4.

Description: The DP4 (Fig. 3D) is unworn. It is rectangular and composed of three lophs oriented perpendicular to the long axis of the tooth, plus a strong posterior cingulum. The pretrite half-lophids show well-developed trefoils. The first pretrite half-loph is high, with a serrated anterior accessory central conule linked to the anterior cingulum, a simple posterior accessory central conule, and a weak mesoconelet. The first posttrite half-loph comprises a mesoconelet and a main conelet, which are subdivided. The second pretrite half-loph has a strong and subdivided anterior accessory central conule and a small and undivided posterior conule. The mesoconelet is nearly absent. The second posttrite half-loph is similar to the first. Both the third pretrite and posttrite half-lophs are similar to the second loph. The posterior cingulum is composed of a row of enamel conules. Small enamel conules are also well developed in the interlophs, which are covered by a thin layer of cementum. Cingula are developed along the anterior margin of the tooth and the lingual side of the first interloph.

The dp3 (Fig. 3E) is broken, and only the posterior part is preserved. The remaining lophid is wide. The pretrite and posttrite half-lophids are rounded and robust. The posterior cingulid is strong and shaped like a thick stick.

The dp4 (Fig. 3E) is narrower and longer than the DP4. It is rectangular and composed of three lophids with strong anterior and posterior cingulids. The first pretrite is trifoliate, with the anterior pretrite central conule linked to the anterior cingulid, whereas the posterior pretrite accessory central conule is individualized and shows a tendency to invade the neighboring entoflexid. The mesoconelet is medium sized. The first posttrite half-lophid has a mesoconelet and weakly outlined anterior and posterior accessory central conules. The second pretrite half-lophid is also trifoliate, with strong anterior and posterior pretrite accessory central conules and a weak mesoconelet. The second posttrite half-lophid has a mesoconelet and an anterior accessory central conule. The third pretrite half-lophid also has a mesoconelet and an anterior pretrite accessory central conule, with the former shifted anteriorly to fuse with the latter. The third posttrite half-lophid has only an anterior mesoconelet. The posterior cingulid is relatively strongly developed, with two main conelets and other smaller conules. Small enamel conules are well developed in the interlophids. The cingulid is developed along the anterior margin of the tooth and the buccal side of the first interlophid.

Comparison: The DP4 appears to erupt from the alveolus. The alternatingly positioned pillars of teeth, subdivision of crown structure, and heavy cementum strongly indicate the genus *Platybelodon*. Six species of *Platybelodon* have been described to date: *P. danovi*, *P. grangeri*, *P. jamandzhalgensis*, *P. beliajevae*, *P. tongxinensis*, and *P. dangheensis* (Wang et al., 2013a). Tobien (1973) suggested that *P. jamandzhalgensis* and *P. danovi* are synonymous. The DP4 of the Kangping specimen is characterized by strong subdivision of crown elements and somewhat strong development of the anterior pretrite central conules, which together are consistent with the diagnosis of *P. grangeri*. Furthermore, *P. dangheensis* is a very early-occurring species with a small size and primitive features. DP4 of *P. tongxinensis* are smaller, whereas *P. beliajevae* has very wide cheek teeth (Wang et al., 2013a). The Kangping specimen is similar to *P. grangeri* in size and morphology. Moreover, its dp3 and dp4 are very similar to those of the *P. grangeri* specimen HMV1813 described by Wang et al. (2013a). Although the new material shows less

wear than HMV1813, the strong lophid and posterior cingulid on dp3, the well-developed trefoils of the pretrite half-lophids, and the medium to weak mesoconelet are identical to the latter. The new material is also similar to HMV1813 in terms of size. The width of the dp3 of HMV1813, estimated from the plate of Wang et al. (2013a), is 23.4 mm, and that of the Kangping material is 25.3 mm. The length and width of dp4 of HMV1813 are 69.5 mm and 30.4 mm, respectively, and those of new material are 72.6 mm and 34.8 mm, respectively. The dimensions of the new material therefore match *P. grangeri* well.

Order PERISSODACTYLA Owen

Family RHINOCEROTIDAE Gill

Subfamily RHINOCEROTINAE Gill

Tribe ELASMOTHERIINI Dollo

Genus *Hispanotherium* Crusafont and Villalta

Hispanotherium wushanense n. sp.

(Fig. 5)

Etymology: specific name, Wushan, the name of the area yielding the holotype.

Holotype: CEESV0032, left maxillary fragment with M2 and M3, belong to an aged individual.

Locality: Kangping.

Age: late middle Miocene, MN7/8.

Referred specimen: CEESV0033, right maxillary fragment with M3.

Diagnosis: Medium-sized *Hispanotherium*, undulated labial wall of upper molars, oval protocone with anterior and posterior constriction grooves, thick cement layer on molars, rectangular M3 with complex secondary folds and strong posterior cingulum.

Description: Part of the facial crest of the upper jaw is preserved (Fig. 5A–C). The anterior tip of the crest is positioned at the level of the anterior half of M2. The crest is robust, and the lateral margin of the ventral surface of the crest has a strong tubercle,

which forms a wide groove between the lateral margin of the crest and the cheek teeth.

M2: The crown surface is rectangular because of the late stage of wear. It is covered with a thick cement layer. The length is less than the width. The protocone is oval with a flat lingual wall, which shows anterior and posterior constriction grooves. The protoloph and metaloph are wide. The crochet is thick and short, and the antecrochet is very large. Their tips connect with each other such that the medifossette is closed. The crista is weak, with three small plications. A small, isolated enamel ring is near the buccal wall of the medifossette. The hypocone connects with the metaloph such that the postfossette is closed.

M3: The protocone has a flat lingual wall and is deeply constricted by the anterior and posterior constriction grooves. The crochet and antecrochet are thick and short. The lingual wall of the medifossette shows undulating secondary folds. The isolated enamel ring in the medifossette, being larger than that of the M2, is close to the buccal wall of the antecrochet. The crista has two folds. The anterior fold is weaker, whereas the posterior fold is very strong. The labial wall of the tooth is not greatly undulated. Being distinct from the M3 of other rhinocerotids, the ectoloph and metaloph are not merged — they run in distinct directions and show an apparent angle. Therefore, the occlusal contour of this tooth is rectangular. The posterior cingulum is very strong. In the holotype, the labial part of the posterior cingulum connects with the ectoloph, and its lingual part is close to the hypocone, which forms a very narrow postfossette that opens posterolingually. However, in the specimen CEESV0033, the posterior cingulum connects with the hypocone, and the labial part is separated from the ectoloph, which makes the postfossette open posterolabially (Fig. 5D).

Comparison: The upper cheek teeth of the Wushan material are medium in size. They have undulated labial walls, oval-shaped protocones with anterior and posterior constriction grooves, and thick cement layers. All of these features indicate that these cheek teeth belong to the genus *Hispanotherium*. Six species of this genus have been reported: *H. materitense*, *H. grimi*, *H. alpani*, *H. corcolence*, *H. lingtongense*, and *H. tunggurense.* According to Deng (2003), *H. grimi* and *H. alpani* can be regarded as

synonyms of *H. materitense.* Sanisidro et al. (2012) also suggested that *H. alpani* is a synonym of *H. materitense*. Cerdeño (1996) indicated that the dental characters of the type material of *H. lintungensis* differ little from those of *H. materitense.* Deng (2003) agreed with this argument and confirmed that *H. lintungensis* is a junior synonym of *H. materitense*. Antoine et al. (2002) established a new species, *H. corcolence*, and listed a series of differences from other species of *Hispanotherium*. However, these features are not stable, and it is difficult to distinguish the cheek teeth characters of *H. corcolence* from those of *H. materitense* based on the figures in Antoine et al. (2002). Therefore, only two valid species, *H. materitense* and *H. tunggurense*, can be compared with the new material of the Yangping locality.

The new material is slightly larger than *H. materitense* (Table 2). The facial crest of *H. materitense* is stronger and more elongated than that of the new material. Its anterior tip extends to the level of the P4/M1 boundary, and is much more elongated than that of the new material (Sanisidro et al., 2012). They share some similarities in cheek teeth, but the protocone of *H. materitense* is longer than that of the new specimens at the same stage of wear. The most significant difference is that the new specimens have strong secondary folds on the median valley of the M3. This character is only found in the advanced elasmotheres. *H. tunggurense* clearly has a larger body size (Table 2) and much stronger undulation of the labial wall on the cheek teeth. Its M3 is triangular, and lacks strong secondary folds (Cerdeño, 1996). Consequently, the features of the new specimens are clearly different from known *Hispanotherium* species, and we therefore establish a new species, *Hispanotherium wushanense* n. sp.

Order ARTIODACTYLA Owen

Family SUIDAE Gray

Subfamily LISTRIODONTINAE Simpson

Genus *Kubanochoerus* Gabunia

Kubanochoerus sp.

(Fig. 6)

Locality: Kangping.

Referred specimens: CEESV0027, left mandible fragment with p2; CEESV0028, mandible fragment with left and right p2 to m2; CEESV0029, maxilary fragment with left P2 to P4; CEESV0031, a broken left M3.

Description: The mandible is robust (Fig. 6). The symphysis is not preserved. It is difficult to determine whether p1 exists; either the diastema between p1 and p2 is very wide, or p1 has been lost. The cheek teeth are bunodont type, and are worn to a very late stage. The teeth are medium in size.

The p2 is elongated from an occlusal view. The labial margin is constricted lingually in the middle, and forms a shallow valley shape. The cingulum is very strong, especially on the anterior and labial margin. The main cusps are worn away, with a nearly quadrilateral cross section remaining with a long tail-shaped posterior horn. The enamel wall on the section is very thick. The p3 is similar to the p2 but larger, and the occlusal surface is wider. The cross section is nearly drop-shaped, and posterior part of the labial wall is constricted lingually. The p4 is almost worn away; the enamel is only preserved on the posterior part of the tooth. The cingulum is thicker than p2 and p3.

The maxillary material is very poorly preserved. It belongs to the same individual as the mandible because they can bite together fully. This material shows that the individual was relatively small and slender.

The M3 is poorly preserved and heavily worn. The occlusal surface only remains in the posterolabial part, but it is clearly identifiable as bunodont-type. The labial cingulum is strong. A wide valley lies between the paracone and metacone, and the ectoconule is absent. The metacone is rounded. A half-circle structure with a very thick enamel wall is in contact with the postcrista. The pentacone is fan-shaped, and the hexacone is large and pointed anterolabially.

Comparison: Although the specimens are damaged and the teeth deeply worn, the characters of the M3 and lower teeth are clearly bunodont. Bunodont listriodonts consist of three genera: *Bunolistriodon*, *Kubanochoerus*, and *Libycochoerus*. The

teeth of *Bunolistriodon* show transitional morphology between lophodont and bunodont listriodonts, and are particularly small (Qiu et al., 1988). In *Libycochoerus*, diastema between p1 and p2 is narrow, and the widths of p4, m1 and m2 exceed their lengths in the middle wear stage (Wilkinson, 1976; Qiu et al., 1988). In *Kubanochoerus*, the diastema between p1 and p2 is wider, and sometimes p1 is missing. The features of the new material are significantly different from the former two genera and fit with those of *Kubanochoerus.* Its size is also similar to that of *Kubanochoerus minheensis*, and significantly smaller than other species of *Kubanochoerus* (Table 3). *K. minheensis* has high main cusps with anterior crests and accessory cusps. The basal parts of the main cusps of the premolars of the new material also show similarity to *K. minheensis*.

Family BOVIDAE Gray

Genus *Turcocerus* Köhler

Turcocerus cf. *kekemaidengensis* Ye et al.

(Fig. 7)

Locality: Kangping.

Geographic distribution: Duolebulejin, Xinjiang; Wushan, Gansu; both in China.

Stratigraphic distribution: late middle Miocene, MN7/8.

Referred specimens: CEESV0001, right maxillary fragment with cheek tooth row; CEESV0002, right maxillary fragment with P4 and M1; CEESV0003, left maxillary fragment with P4 to M2; CEESV0004, left maxillary fragment with P4 to broken M3; CEESV0005, left maxillary fragment with M2 and M3; CEESV0006, left maxillary fragment with P3 and P4; CEESV0007, left maxillary fragment with M1 and M2; CEESV0008, right maxillary fragment with P4 to broken M2; CEESV0009, right maxillary fragment with broken M2 and M3; CEESV0010, left P2; CEESV0011, left M3; CEESV0012, left M3; CEESV0013, left mandible fragment with p3 and p4; CEESV0014, right mandible fragment with p4 to m2; CEESV0015, right mandible

fragment with p4 to m2; CEESV0016, left mandible fragment with m2 to m3; CEESV0017, left mandible fragment with p4, m1, and m3; CEESV0018, left mandible fragment with m1; CEESV0019, left mandible fragment with m2 and m3; CEESV0020, right mandible fragment with m3; CEESV0021, right p2; CEESV0022, right p3; CEESV0023, broken left m3.

Description: Cheek teeth of these specimens are hypsodont. The P2 is small, and the length is larger than the width. The paracone is prominent and close to the parastyle. In buccal view, the ribs of the paracone and the parastyle are closely juxtaposed and tend to be fused at the base. The metacone is weak without a rib. The metastyle also is not prominent. The anterior and posterior parts of protocone are equally developed with a median lingual groove.

The P3 is similar to the P2, but is larger and anteroposteriorly compressed. The anterior and posterior parts of the protocone are more closely positioned with a shallower median lingual groove than those of P2.

The P4 is larger than the P3, and is triangular. The para- and metacones are nearly fused without a rib in buccal view. Both para- and metastyles are prominent with strong ribs in buccal view. The protocone is singular. Folds are developed on the posterolingual crista. In some specimens, a small enamel ring is formed in this position.

The M1 is rectangular to square. The parastyle is rounded and has a strong rib on the buccal wall. The mesostyle is sharp and oriented to the anterobuccal side. It also has a strong rib on the buccal wall. The paracone is bulky. The metastyle extends posteriorly, but it is relatively weak. The metacone is also bulky, but without a rib. The anterior angles of central cavities are always very close to the buccal wall. The lingual walls of the protocone and metaconule are rounded. The entostyle is strong.

The M2 is larger and longer than M1. The width of the crown narrows considerably upward. The parastyle is sharp, with a rib stronger than that of M1; and the mesostyle is sharp and extended buccally. The lingual wall of the protocone is angular. The other features are similar to those of M1. The entostyle is weaker than that of M1.

The M3 is similar to M2, except that the posterior lobe of the M3 is slightly narrower than the anterior lobe.

The p2 is very small. The parastylid is not separated from the paraconid. The protoconid is high. The transverse cristid is strongly posterolingually oblique. The hypoconid is low and small. The posterior valley is almost enclosed by the posterior cristid and the entostylid.

The p3 is larger and higher than the p2. The parastylid is branched from the paraconid. The protoconid is large and high, and the transverse cristid is also strongly posterolingually oblique. However, no metaconid is observed. The hypoconid is buccally convex, separated from the protoconid by a buccal groove. The posterior cristid and the entostylid do not enclose the back valley. The distal end of the entostylid is somewhat inflated.

The p4 is slightly larger than the p3. The parastylid and the paraconid are well-branched. The protoconid is also large and high, but the transverse cristid is not as posterolingually oblique as those of the p2 and p3. The metaconid has been individualized from the transverse cristid; however, there is no anterolingual cristid. The groove between the protoconid and hypoconid is more developed than that of the p3. The hypoconid is buccally convex, and the posterior cristid and entostylid do not enclose the back valley.

The m1 is rectangular. The parastylid and entostylid are moderately developed, but the metastylid is nearly absent. The entostylid is relatively strong. The metaconid and entoconid are moderately bulky. They are sharp in lingual view, and lingual ribs are nearly absent. The anterior cingulid (goat fold) is developed. The protoconid and hypoconid are strongly buccally convex.

The m2 has a similar morphology to that of m1, although it is more anteroposteriorly elongated and higher crowned. The parastylid and entostylid are moderately developed, and the metastylid and lingual ribs of the metaconid and entoconid are very weak or absent. The lingual wall of the tooth shows an apparent undulated structure; the postmetacristid fully covers the preentocristid lingually. The anterior cingulid (goat fold) is even stronger, but the entostylid is weaker than those of

m1.

The m3 is even higher crowned. In the early stage of wear, the metastylid is present, and the entostylid shows complex plication; however, their morphology becomes more similar in the slightly deep wear stage. The step structure of the lingual wall is more prominent than that of the m2, and the hypoconid appears less convex than that of the m1 and m2. The entoconid is even weaker than those of the m1 and m2. The third lobe is composed only of the hypoconulid, without the entoconulid. It is narrow and triangular, originates from the posterobuccal wall of the posthypocristid, and extends posteriorly and slightly buccally.

Comparison: The hypsodont crowns, strongly reduced premolars, and the absence of an anteriorly extending metaconid of p4 support attributing these teeth to the Bovidae. Because of the medium size, hypsodonty, sharp cusps, strong goat folds, and the undulated lingual wall of the lower molars, we have identified these specimens as belonging to the genus *Turcocerus*, which was widely distributed from the early to middle Miocene of Asia.

To date, reported species of *Turcocerus* include *T. jiulongkouensis*, *T. robustus*, *T. stenocephalus*, *T. grangeri*, *T. noverca*, *T. kekemaidengensis*, and *T. gracile*. *Turcocerus* is characterized by its slightly helical (about one fourth of a circle) horn cones, and the species are distinguishable from each other based on the morphology of their pedicles and horn cones. Because there is no horn cone in the new material, we identify these teeth at the species level based mainly on size. The dimensions of the teeth fit well with *T. kekemaidengensis* (Table 4). The teeth of *T. jiulongkouensis*, *T. robustus*, and *T. stenocephalus* are much larger than the new material; in contrast, those of *T. noverca* are clearly smaller than the new material. Furthermore, although the features on the cheek teeth are not easily distinguishable between the different species, those of the new material are nearly identical with those of the holotype of *T. kekemaidengensis* from the Duolebulejin locality, which indicates a very close relationship between these species. For example, in *T. kekemaidengensis*, the ectostylids of the m3 are weaker than those of the m1 and m2 (Ye et al., 1999). However, considering the absence of a horn core, we refer to these specimens as

Turcocerus cf. *kekemaidengensis*.

5. Discussion

5.1. Age

The Kangping locality on the eastern wing of the syncline is closer to the core than the Nanyu locality on the western wing. The stratigraphic correlation indicates that the Kangping fauna is younger than the Nanyu fauna, and the Yangping fauna is located at the base of the succession (Fig. 2). The Kangping fauna was correlated with MN7/8. *Platybelodon grangeri*, in the Kangping fauna, has been found in several other mammalian faunas of MN7/8, including the Tunggur, Inner Mongolia, Zengjia and Laogou, Gansu (Deng et al., 2007, 2013; Wang, 2014). *Kubanochoerus* sp. is most similar to *K. minheensis*. Only a single definite record of *K. minheensis* has been reported, from the Xianshuihe Formation of the Xining Basin, Qinghai (Qiu et al., 1981). Qiu et al. (1981) indicated that this fauna can be correlated with the Tunggur, Inner Mongolian fauna, which is a characteristic fauna of MN7/8. Ye (1989) reported that *Kubanochoerus* sp., found in Duolebulejin, was very similar to *K. minheensis*. *Turcocerus kekemaidengensis* was a member of the Kekemaideng fauna in Duolebulejin (Ye et al., 1999), and this fauna has been correlated with MN7/8 (Deng et al., 2007; Deng, 2016). Moreover, the Kangping fauna contains a highly derived species of *Hispanotherium*, which is more derived than *H. materitense*; the latter was widespread in the MN6 faunas of China (Deng, 2003; Deng et al., 2007, 2013). The appearance of *H. materitense* extended even to MN7/8 in Laogou, Gansu (Deng et al., 2013). Therefore, the Kangping fauna can be regarded as another typical fauna of MN7/8.

The fauna of the Nanyu locality correlated with MN6. Wang et al. (2013b) reported the occurrence of *Gomphotherium wimani* and inferred a middle Miocene age. Our new material includes an m3 and a humerus of *Platybelodon* aff. *tongxinensis*, which is representative in faunas of MN6 in China, such as the Dingjiaergou Fauna in Tongxin, Ningxia (Deng et al., 2007) and Shinanu, Gansu

(Wang, 2014).

The horizon of the Yangping section is much lower than that of the Nanyu fauna (Fig. 2), and this section is early Miocene in age, as indicated by presence of cf. *Gomphotherium* sp., a primitive gomphothere. Based on paleomagnetic dating (unpublished data), the age of the Yangping strata is 21–20 Ma. This site therefore represents the earliest record of proboscideans not only in China but also in all of East Asia; as it predates the occurrences of *Gomphotherium annectens* in the Lower Hiramaki Formation (18.2 Ma) in Japan (Tomida et al., 2013) and proboscidean material from Zhangjiaping (approximately 19.5 Ma) (Qiu et al., 2013). Therefore, the Yangping material defines the "Proboscidean Datum Event" well (Tassy, 1990). This event is helpful for establishing the Shanwangian Stage in East Asia, which can be correlated with the marine Burdigadian beginning at 20.44 Ma. The Yangping Locality is also suitable for selection as the lower boundary stratotype of the Shanwangian.

5.2. Evolutionary trends

Comparison between the same mammalian lineage from MN6 and MN7/8 shows evolutionary trends within several groups. Ye and Jia (1986) indicated that the degree of hypsodonty and the molar length/width ratio of *Platybelodon grangeri* from MN7/8 are both higher than those of *P. tongxinensis* from MN6. Our material shows that the humerus of *P. tongxinensis* from the Nanyu fauna is very slender (Fig. 4, Table 1). Wang et al (2016a) listed measurements of proboscidean limbs; the approximate ratio of the minimum width to the maximum length of the shaft for *P. grangeri* is approximately 0.124 (Table 1). Because the new humerus of *P. tongxinensis* has a broken lateral tuberosity, only the length between the head and the distal articulation could be measured. The ratio of the minimum width of the shaft to this length is approximately 0.118 (Table 1). This ratio would be lower if the maximum length were available. However, it is clear that *P. tongxinensis* has a more slender humerus than does *P. grangeri*. Standing posture has been investigated in several studies. With increasing body mass, more derived taxa may have developed

thicker limb bones to support greater weight. This trend was likely present in *Platybelodon*.

Both the new taxa *H. wushanense* and the almost contemporary species *H. tungurense* were larger than *H. materitense*, which was the first to appear in China in MN6 (Cerdeño, 1996; Deng, 2003). *H. wushanense* also has a prominent derived character in its secondary plication folds on M3. Early elasmotheres such as *Ningxiatherium* that lived in the early Late Miocene still lacked secondary folds (Antoine et al., 2002; Deng, 2008). Only late and highly derived members of this clade, such as *Elasmotherium*, have strong secondary folds on their cheek teeth (Tong et al., 2014; Schvyreva, 2015). Therefore, these folds are a clear example of parallel evolution. *Hispanotherium* originated from Europe (Sanisidor et al., 2012). *H. materitense* was widespread in Europe in MN4−5 and spread to China in MN6 (Deng, 2003). By MN7/8, two members of *Hispanotherium* more derived than *H. matriense* occurred in China, initiated evolutionary divergence. *H. tunggurense* was considerably larger, whereas *H. wushanense* had highly specialized characters. This phenomenon has been noted in other perissodactyl taxa. For example, in the hipparion horse genus *Plesiohipparion*, two most derived species were *Plesiohipparion shanxiense* and *Plesiohipparion huangheense*, each of which had clearly derived features: large size and a highly specialized pattern on the lower cheek teeth, respectively (Qiu et al., 1987; Bernor et al., 2015). The growth of within-genus diversity was likely influenced by the climate and environmental improvement. Some authors have proposed the occurrence of global climate change from the middle to late middle Miocene. Lewis et al. (2006) detected a thermal transition in Antarctica in the middle Miocene with a series of temperature drop events, the most recent of which likely occurred between 13.62 and 12.44 Ma. Domingo et al. (2009, 2012) found that the paleontological record of Spain corresponded with global decrease in temperature and increase in aridity in 14.1−13.8 Ma. Böhme et al. (2007) reached a similar conclusion from the analysis of fossil wood flora in Germany. European authors argued that *H. materitense* lived in arid conditions (Cerdeño and Nieto, 1995; Iñigo and Cerdeño, 1997). However, Deng (2003) indicated that *Hispanotherium* is

consistently found together with members of the Amebelodontidae, which may show a tendency to live near water. The fluvial gray-to-yellowish sandstones with gravel in the strata that yielded *H. materitense* are consistent with this argument. Therefore, the paleoenvironment of *H. materitense* in China is somewhat different from that of the same species in Europe. Palynological data for the Tianshui Basin were interpreted to indicate a relatively warm and humid environment in the middle Miocene (Hui et al., 2011). In summary, global climate change influenced the environment of Europe, but affected China to a lesser degree. *Hispanotherium* likely migrated east and ultimately settled in China. The favorable environment promoted diverse evolutionary trends for *Hispanotherium*. The evolution of *Plesiohipparion* was consistent with the same principle. The climate of the Pliocene began to change incrementally in a setting of global warming (Dowsett et al., 2010; Haywood et al., 2010, 2013). *Plesiohipparion* lived in a suitable environment, and therefore the diversity of *Plesiohipparion* was increased.

After Qiu et al. (1981) first discovered *Kubanocerus minheensis* in China, a series of discoveries of small-sized bunodont listriodont fossils were reported from successions of several localities. Ye (1989) found *Kubanocerus* material in Duolebulejin, Xinjiang and argued that this species is most similar to *K. minheensis* based on body size and features. Ye et al. (1992) also reported *Bunolistriodon intermedius* found in Tongxin, Ningxia. We have now found material similar to *K. minheensis* in Wushan, Gansu. The large-sized members of *Kubanocerus* were dominant suids in the middle Miocene in China (Deng et al., 2007, 2013), and the small-sized bunodont-type listriodonts began to disperse from MN6 to MN7/8. After the occurrence of *Kubanocerus*, *Listriodon* began to disperse across Eurasia (Deng et al., 2007, 2013; Deng, 2016). This genus has lophodont cheek teeth, and species of this genus are universally smaller than the bunodont listriodonts (Chen, 1986). We infer that the size of listriodonts displayed miniaturization since MN6 in China. The reason for this phenomenon was likely changes of climate or ecological niches. Deng (2016) indicated that *Kubanocerus* lived in interforest open field, whereas *Listriodon* lived in shrublands; the lophodont teeth of *Listridon* were adapted for hard vegetation.

5.3. Paleozoogeography

Genus *Turcocerus* is a representative bovid taxon of the middle Miocene in China. As mentioned above, *Turcocerus* was distributed very widely in China from east to west. The main locality of *Turcocerus* in eastern China is the Jiulongkou area; that in the middle is the Tunggur area; and those in the west are the Tongxin, Duolebulejin, and Xining areas. The eastern species in the Jiulongkou area, including *T. jiulongkouensis*, *T. robustus*, and *T. stenocephalus*, were all large in size. The western species, *T. noverca* from the Xining Basin, *T. kekemaidengensis* from Duolebulejin and Kangping, and *Turcocerus* sp. 2 from Tongxin (which has similar dimensions to *T. kekemaidengensis*, see Wang et al., 2016b), were all small in size. In contrast, in Tunggur, a larger species, *T. grangeri*, and a smaller species, *T. noverca*, were both found in horizons of the same age (Wang et al., 2003). The distribution of the Middle Miocene suids in China was interesting. The small-sized bunodont listriodonts began to disperse from MN6 to MN7/8. The main localities for this group are the Xining Basin, Qinghai (Qiu et al., 1981); Tongxin, Ningxia (Ye et al., 1992) and the Wushan Subbasin, Gansu, all of which are in western China. This situation is very similar to that for *Turcocerus*.

Deng et al. (2011) proposed a major boundary of eastern and western zoogeographic differentiation. This proposed boundary would have extended south-southwest along the eastern margin of the Taihang Mountains and reached the eastern margins of the Wudang–Shennongjia Mountains across the Yellow River before the end of the middle Miocene. In the faunas found to the east of this boundary, abundant, low-crowned cervids lived in forests, whereas in the faunas to the west of the boundary, large numbers of typical high-crowned bovids lived in open environments. Deng (2009, 2016) indicated that the richness of large-sized mammals represents a closed environment. The large-sized *Turcocerus* and suids likely indicate closed environments, and their smaller-sized counterparts reveal open environments. This inference is consistent with the boundary proposed by Deng et al. (2011) based on the distribution of these localities. However, Tunggur is relatively unique among

these localities. Both the larger *T. grangeri* and the smaller *T. noverca* were found here at the same horizon (Pilgrim, 1934; Wang et al., 2003). Zhang et al. (2011) argued that the faunal community structure and continuity of the main lineages of Damiao, which is geographically near Tunggur, suggest a relatively stable moderate, humid and warm forest–grassland environment from the early Miocene to early late Miocene. Tunggur was likely also a transitional area similar to Damiao, with a diverse environment that would have provided suitable habitats for these two species with significantly different body sizes. This finding also suggests that in the middle Miocene, the biogeographic boundary in Inner Mongolia was less rigid, and that a large transitional area likely existed.

Acknowledgements

We thank Prof. Tao Deng for his useful discussion. We thank Yu Chen for his sketch and providing literature. We thank Dan Su for the preparation of the specimen and Wei Gao for photographing. We thank Ben-Hong Guo, Hao Yu and Qiang-Qiang Wang for their field work support. We thank the reviewer Dr. Kimura Yuri and the editor Si-Wei Chen for their review and important comments for our manuscript. This work was supported by the Strategic Priority Cultivating Research Program, CAS (Grant No. XDPB05), and the Key Research Program of Frontier Sciences, CAS, the National Natural Science Foundation of China (Grant Nos. 41671001, 41330745, 41372001, 41430102), the Special Research Program of Basic Science and Technology of the Ministry of Science and Technology (Grant No. 2015FY310100-14), and all China Commission of Stratigraphy Project (Grant No. DD20160120-04). The first author acknowledges funding from the China Scholarship Council for 1 year research in the Bernor Lab at Howard University.

References

Andrews, R.C., 1932. The new conquest of Central Asia, a narrative of the explorations of the Central Asiatic Expeditions in Mongolia and China, Natural History of Central Asia. American Museum of Natural History 1, 1–678.

Antoine, P.O., Alférez, F., Iñigo, C., 2002. A new elasmotheriine (Mammalia, Rhinocerotidae) from the Early Miocene of Spain. Comptes Rendus Palevol 1 (1), 19–26.

Bernor, R.L., Sun, B.Y., Chen, Y., 2015. *Plesiohipparion shanxiense* n. sp. from the Early Pleistocene (Nihowanian) of E Shanxi, China. Bollettino della Società Paleontologica Italiana 54 (3), 197–210.

Böhme, M., Bruch, A.A., Selmeier, A., 2007. The reconstruction of Early and Middle Miocene climate and vegetation in Southern Germany as determined from the fossil wood flora. Palaeogeography, Palaeoclimatology, Palaeoecology 253 (1–2), 91–114.

Cao, Z.X., Du, H.J., Zhao, Q.Q., Cheng, J., 1990. Discovery of the Middle Miocene fossil mammals in Guanghe district, Gansu and their stratigraphic significance. Geoscience 4 (2), 16–29.

Cerdeño, E., 1996. Rhinocerotidae from the Middle Miocene of the Tunggur Formation, Inner Mongolia (China). American Museum Novitates 3184, 1–43.

Cerdeño, E., Nieto, M., 1995. Evolution of Rhinocerotidae in Western Europe: influence of climatic changes. Paleogeography, Paleoclimatology, Paleoecology 114, 325–338.

Chen, G.F., 1986. A new species of *Listriodon* Meyer (Suidae, Artiodactyla, Mammalia) from Xin'an, Henan. Vertebrata PalAsiatica 24 (4), 295–307 (in Chinese, with English summary).

Chen, G.F., Wu, W.Y., 1976. Miocene mammalian fossils of Jiulongkou, Cixian District, Hebei. Vertebrata PalAsiatica 14 (1), 6–15 (in Chinese).

Deng, T., 2003. New material of *Hispanotherium materitense* (Rhinocerotidae, Perissodactyla) from Laogou of Hezheng County (Gansu, China), with special reference to the Chinese Middle Miocene elasmotheres. Geobios 36 (2), 141–150.

Deng, T., 2004a. A new species of the rhinoceros *Alicornops* from the Middle Miocene of the Linxia Basin, Gansu, China. Paleontology 47 (6), 1427–1439.

Deng, T., 2004b. Establishment of the Middle Miocene Hujialiang Formation in the

Linxia Basin of Gansu and its features. Journal of Stratigraphy 28 (4), 307–312 (in Chinese, with English abstract).

Deng, T., 2008. A new elasmothere (Perissodactyla, Rhinocerotidae) from the Late Miocene of the Linxia Basin in Gansu, China. Geobios 41 (6), 719–728.

Deng, T., 2009. Late Cenozoic environmental change in the Linxia Basin (Gansu, China) as indicated by mammalian cenograms. Vertebrata PalAsiatica 47 (4), 282–298.

Deng, T., 2011. Diversity variations of the Late Cenozoic mammals in the Linxia Basin and their response to the climatic and environmental backgrounds. Quaternary Sciences 31 (4), 577–588 (in Chinese, with English abstract).

Deng, T., 2016. Record and characteristics of the mammalian faunas of Northern China in the Middle Miocene climatic optimum. Quaternary Sciences 36 (4), 810–819 (in Chinese, with English abstract).

Deng, T., Hou, S.K., Wang, H.J., 2007. The Tunggurian Stage of the continental Miocene in China. Acta Geologica Sinica 81 (5), 709–721.

Deng, T., Liang, Z., Wang, S.Q., Hou, S.K., Li, Q., 2011. Discovery of a Late Miocene mammalian fauna from Siziwang Banner, Inner Mongolia and its paleozoogeographical significance. Chinese Science Bulletin 56 (6), 526–534.

Deng, T., Qiu, Z.X., Wang, B.Y., Wang, X.M., Hou, S.K., 2013. Late Cenozoic biostratigraphy of the Linxia Basin, northwestern China. In: Wang, X.M., Flynn, L.J., Fortelius, M. (Eds.), Fossil Mammals of Asia: Neogene Biostratigraphy and Chronology. Columbia University Press, New York, pp. 243–273.

Domingo, L., Cuevas-González, J., Grimes, S.T., Fernández, M.H., López-Martínez, N., 2009. Multiproxy reconstruction of the palaeoclimate and palaeoenvironment of the Middle Miocene Somosaguas site (Madrid, Spain) using herbivore dental enamel. Palaeogeography, Palaeoclimatology, Palaeoecology 272 (1–2), 53–68.

Domingo, L., López-Martínez, N., Grimes, S.T., 2012. Trace element analyses indicative of paleodiets in Middle Miocene mammals from the Somosaguas site (Madrid, Spain). Geologica Acta 10 (3), 239–247.

Dong, W., 1987. Miocene mammalian fauna of Xiaolongtan, Kaiyuan, Yunnan

Province. Vertebrata PalAsiatica 25 (2), 116–123 (in Chinese, with English summary).

Dowsett, H.J., Robinson, M., Haywood, A.M., Salzmann, U., Hill, D.J., Sohl, L., Chandler, M.A., Williams, M., Foley, K., Stoll, D., 2010. The PRISM3D Paleoenvironmental Reconstruction. Stratigraphy 7, 123–139.

Gentry, A.W., 1992. The subfamilies and tribes of the family Bovidae. Mammal Review 22 (1), 1–32.

Guan, J., 1988. The Miocene strata and mammals from Tongxin, Ningxia and Guanghe, Gansu. Memoirs of Beijing Natural History Museum 42, 1–21 (in Chinese, with English abstract).

Haywood, A.M., Dowsett, H.J., Otto-Bliesner, B., Chandler, M.A., Dolan, A.M., Hill, D.J., Lunt, D.J., Robinson, M.M., Rosenbloom, N., Salzmann, U., Sohl, L.E., 2010. Pliocene Model Intercomparison Project (PlioMIP): experimental design and boundary conditions (Experiment 1). Geoscientific Model Development 3, 227–242.

Haywood, A.M., Hill, D.J., Dolan, A.M., Otto-Bliesner, B., 2013. Large-scale features of Pliocene climate: results from the Pliocene Model Intercomparison Project. Climate of the Past 8 (4), 191–209.

Hui, Z.C., Li, J.J., Xu, Q.H., Song, C.H., Zhang, J., Wu, F.L., Zhao, Z.J., 2011. Miocene vegetation and climatic changes reconstructed from a sporopollen record of the Tianshui Basin, NE Tibetan Plateau. Palaeogeography, Palaeoclimatology, Palaeoecology 308, 373–382.

Iñigo, C., Cerdeño, E., 1997. The *Hispanotherium materitense* (Rhinocerotidae) from Corcoles (Guadalajara, Spain): its contribution to the systematics of the Miocene Iranotheriina. Geobios 30, 243–266.

Lewis, A.R., Marchant, D.R., Ashworth, A.C., Hemming, S.R., Machlus, M.L., 2006. Major middle Miocene global climate change: Evidence from East Antarctica and the Transantarctic Mountains. Geological Society of America Bulletin 119 (11–12), 1449–1461.

Li, C.K., Qiu, Z.D., Wang, S.J., 1981. Discussion on Miocene stratigraphy and

mammals from Xining Basin, Qinghai. Vertebrata PalAsiatica 19 (4), 313–320 (in Chinese, with English abstract).

Liu, D.S., Ding, M.L., Gao, F.Q., 1960. The Cenozoic stratigraphical sections between Xi'an and Lantian. Chinese Journal of Geology (4), 199–208 (in Chinese).

Pilgrim, G.E., 1934. Two new species of sheep-like antelope from the Miocene of Mongolia. American Museum Novitates 716, 1–29.

Qiu, Z.D., 2000. Insectivore, dipodoidean and lagomorph from the Middle Miocene Quantougou Fauna of Lanzhou, Gansu. Vertebrata PalAsiatica 38 (4), 287–302 (in Chinese, with English summary).

Qiu, Z.D., 2001a. Cricetid rodents from the Middle Miocene Quantougou Fauna of Lanzhou, Gansu. Vertebrata PalAsiatica 39 (3), 204–214.

Qiu, Z.D., 2001b. Glirid and gerbillid rodents from the Middle Miocene Quantougou Fauna of Lanzhou, Gansu. Vertebrata PalAsiatica 39 (4), 297–305.

Qiu, Z.D., Li, C.K., 2003. Rodents from the Chinese Neogene: Biogeographic relationships with Europe and North America. Bulletin of the American Museum of Natural History 279, 586–602.

Qiu, Z.D., Li, C.K., Wang, S.J., 1981. Miocene mammalian fossils from Xining Basin, Qinghai. Vertebrata PalAsiatica 19 (2), 156–173 (in Chinese, with English summary).

Qiu, Z.D., Wang, X.M., Li, Q., 2006. Faunal succession and biochronology of the Miocene through Pliocene in Nei Mongol (Inner Mongolia). Vertebrata PalAsiatica 44 (2), 164–181.

Qiu, Z.D., Wang, X.M., Li, Q., 2013. Neogene fauna succession and biochronology of Central Nei Mongol (Inner Mongolia). In: Wang, X.M., Flynn, L.J., Fortelius, M. (Eds.), Fossil Mammals of Asia: Neogene Biostratigraphy and Chronology. Columbia University Press, New York, pp. 155–186.

Qiu, Z.X., Qiu, Z.D., 1990. Neogene local mammalian faunas: Succession and ages. Journal of Stratigraphy 14 (4), 241–260 (in Chinese, with English abstract).

Qiu, Z.X., Qiu, Z.D., 1995. Chronological sequence and subdivision of Chinese

Neogene mammalian faunas. Palaeogeography, Palaeoclimatology, Palaeoecology 116, 41–70.

Qiu, Z.X., Wang, B.Y., 2007. Paracerathere fossils of China. Palaeontologia Sinica, New Series C 29, 1–396 (in Chinese, with English summary).

Qiu, Z.X., Huang, W.L., Guo, Z.H., 1987. The Chinese hipparionine fossils. Palaeontologia Sinica, New Series C 25, 1–250 (in Chinese, with English summary).

Qiu, Z.X., Ye, J., Huo, F.C., 1988. Description of a *Kubanochoerus* skull from Tongxin, Ningxia. Vertebrata PalAsiatica 26 (1), 1–19 (in Chinese, with English summary).

Sanisidro, O., Alberdi, M.T., Morales, J., 2012. The first complete skull of *Hispanotherium materitense* (Prado, 1864) (Perissodactyla, Rhinocerotidae) from the middle Miocene of the Iberian Peninsula. Journal of Vertebrate Paleontology 32 (2), 446-455.

Schvyreva, A.K., 2015. On the importance of the representatives of the genus Elasmotherium (Rhinocerotidae, Mammalia) in the biochronology of the Pleistocene of Eastern Europe. Quaternary International 379, 128–134.

Sisson, S., 1953. The Anatomy of the Domestic Animals. W. B. Saunders Company, Philadelphia, 972 pp.

Spock, L.E., 1929. Pliocene beds of the Iren Gobi. American Museum Novitates 394, 1–8.

Tassy, P., 1990. The “proboscidean datum event”: how many proboscideans and how many events? In: Lindsay, E.H., Fahlbusch, V., Mein, P. (Eds.), European Neogene Mammal Chronology. Plenum Press, New York, pp. 237–252.

Tassy, P., 2014. L’odontologie de *Gomphotherium angustidens* (Cuvier, 1817) (Proboscidea, Mammalia): données issues du gisement d’En Péjouan (Miocène moyen du Gers, France). Geodiversitas 36 (1), 35–115.

Tobien, H., 1973. The structure of the mastodont molar (Proboscidea, Mammalia). Part 1: The bunodont patterns. Mainzer Geowissenschuftliche Mitteilungen 2, 115–147.

Tomida, Y., Nakaya, H., Saegusa, H., Miyata, K., Fukuchi, A., 2013. Miocene land mammals and stratigraphy of Japan. In: Wang, X.M., Flynn, L.J., Fortelius, M. (Eds.), Neogene Terrestrial Mammalian Biostratigraphy and Chronology of Asia. Columbia University Press, New York, pp. 314–333.

Tong, H.W., Wang, F.G., Zheng, M., Chen, X., 2014. New Fossils of *Stephanorhinus kirchbergensis* and *Elasmotherium peii* from the Nihewan Basin. Acta Anthropologica Sinica 33 (3), 369–388 (in Chinese, with English abstract).

van der Made, J., 1996. Listriodontinae (Suidae, Mammalia), their evolution, systematics and distribution in time and space. Contribution to Tertiary and Quaternary Geology 33, 3–254.

Wang, S.Q., 2014. *Gomphotherium inopinatum*, a basal *Gomphotherium* species from the Linxia Basin, China, and other Chinese members of the genus. Vertebrata PalAsiatica 52 (2), 183–200.

Wang, S.Q., Ye, J., 2015. Paleobiological implications of new material of *Platybelodon danovi* from the Dingjiaergou Fauna, western China. Historical Biology 27 (8), 987–997.

Wang, S.Q., He, W., Chen, S.Q., 2013a. Gomphotheriid mammal *Platybelodon* from the Middle Miocene of Linxia Basin, Gansu, China. Acta Palaeontologica Polonica 58 (2), 221–240.

Wang, S.Q., Liu, S.P., Xie, G.P., Liu, J., Peng, T.J., Hou, S.K., 2013b. *Gomphotherium wimani* from Wushan County, China, and its implications for the Miocene stratigraphy of the Tianshui area. Vertebrata PalAsiatica 51 (1), 71–84.

Wang, S.Q., Shi, Q.Q., Hui, Z.C., Pang, T.J., 2015. Diversity of Moschidae (Ruminantia, Artiodactyla, Mammalia) in the Middle Miocene of China. Paleontological Research 19 (2), 143–155.

Wang, S.Q., Shi, Q.Q., He, W., Chen, S.Q., Yang, X.W., 2016a. A new species of the tetralophodont amebelodontine *Konobelodon* Lambert, 1990 (Proboscidea, Mammalia) from the Late Miocene of China. Geodiversitas 38 (1), 65–97.

Wang, S.Q., Zong, L.Y., Yang, Q., Sun, B.Y., Li, Y., Shi, Q.Q., Yang, X.W., Ye. J., Wu, W.Y., 2016b. Biostratigraphic advance of subdividing the Neogene Dingjiaergou

mammalian fauna in Tongxin County, Ningxia Province, and its background for the uplift of the Tibetan Plateau. Quaternary Sciences 36 (4), 789–809 (in Chinese, with English abstract).

Wang, X.M., Qiu, Z., Opdyke, N.D., 2003. Litho-, bio-, and magnetostratigraphy and paleoenvironment of Tunggur Formation (Middle Miocene) in central Inner Mongolia, China. American Museum Novitates, 1–31.

Wang, X.M., Qiu, Z.D., Li, Q., Wang, B.Y., Qiu, Z.X., Downs, W.R., Xie, G.P., Xie, J.Y., Deng, T., Takeuchi, G.T., Tseng, Z.J., Chang, M.M., Liu, J., Wang, Y., Biasatti, D., Sun, Z.C., Fang, X.M., Meng, Q.Q., 2007. Vertebrate paleontology, biostratigraphy, geochronology, and paleoenvironment of Qaidam Basin in northern Tibetan Plateau. Palaeogeography, Palaeoclimatology, Palaeoecology 254(3/4), 363–385.

Wilkinson, A.F., 1976. The lower Miocene Suidae of Africa. Fossil Vertebrates of Africa 4, 173–282.

Wu, W.Y., Ye, J., Meng, J., Bi, S.D., Liu, L.P., Zhang, Y., 1998. Progress of the study of Tertiary biostratigraphy in North Junggar Basin. Vertebrata PalAsiatica 36 (1), 24–31 (in Chinese, with English summary).

Wu, W.Y., Meng, J., Ye, J., 2003. The discovery of *Pliopithecus* from northern Junggar Basin, Xinjiang. Vertebrata PalAsiatica 41 (1), 76–86.

Yan, D.F., 1979. Einige der fossilen Miozänen säugetiere der keris von Fangxian in der Provinz Hupei. Vertebrata PalAsiatica 17 (3), 189–199 (in Chinese, with Germen summary).

Ye, J., 1989. Middle Miocene artiodactyls from the northern Junggar Basin. Vertebrata PalAsiatica 27 (1), 37–52 (in Chinese, with English summary).

Ye, J., Jia, H., 1986. *Platybelodon* (Proboscidea, Mammalia) from the Middle Miocene of Tongxin, Ningxia. Vertebrata PalAsiatica 24 (2), 139–151 (in Chinese, with English summary).

Ye, J., Qiu, A.X., Zhang, G.D., 1992. *Bunolistriodont intermedius* (Suidae, Artiodactyla) from Tongxin, Ningxia. Vertebrata PalAsiatica 30 (2), 135–145 (in Chinese, with English summary).

Ye, J., Wu, W.Y., Bi, S.D., Zhang, Y., Meng, J., 1999. A new species of *Turcocerus* from the Middle Miocene of the northern Junggar Basin. In: Wang, Y.Q., Deng, T. (Eds.), Proceedings of the Seventh Annual Meeting of the Chinese Society of Vertebrate Paleontology. China Ocean Press, Beijing, pp. 149–156 (in Chinese, with English abstract).

Ye, J., Wu, W.Y., Meng, J., 2001. The age of Tertiary strata and mammal faunas in Ulungur River area of Xinjiang. Journal of Stratigraphy 25 (4), 283–287 (in Chinese, with English abstract).

Zachos, J., Pagani, M., Sloan, L., Thomas, E., Billups, K., 2001. Trends, rhythms, and aberrations in global climate 65 Ma to present. Science 292 (5517), 686–693.

Zhang, Z.Q., Wang, L.H., Kaakinen, A., Liu, L.P., Fortelius, M., 2011. Miocene mammalian faunal succession from Damiao, central Nei Mongol and the environmental changes. Quaternary Sciences 31 (4), 608–613 (in Chinese, with English abstract).

Zhang, Z.S., Guo, Z.T., 2005. Spatial character reconstruction of different periods in Oligocene and Miocene. Quaternary Sciences 25 (4), 523–530 (in Chinese, with English abstract).

Figures

Fig. 1. Map showing fossil localities in the Wushan Subbasin, Gansu, western China.

Fig. 2. Geological section of fossil localities.

Fig. 3. Fossils of proboscideans from the Wushan Subbasin. (A, B) Molar fragment of cf. *Gomphotherium* sp., CEESV0034, in occlusal (A) and lateral (B) views. (C) Occlusal view of right m3 of *Platybelodon* aff. *tongxinensis*, CEESV0025. (D) Occlusal view of right DP4 of *Platybelodon grangeri*, CEESV0024. (E) Occlusal view of left dp3 and dp4 of *Platybelodon grangeri*, CEESV0037. Scale bar for all teeth = 5 cm. (F, G) Right humerus of *Platybelodon* aff. *tongxinensis*, CEESV0026, in caudal (F) and cranial (G) views; scale bar = 10 cm.

Fig. 4. Size comparison of humerus of proboscideans, modified from Wang et al. (2016a).

Fig. 5. *Hispanotherium wushanense* n. sp. (A–C) Holotype, left maxillary fragment with M2 to M3, CEESV0032, in occlusal view with photo (A) and sketch (B) and in labial view (C). (D) Sketch in occlusal view of right M3, CEESV0033. Scale bar = 5 cm.

Fig. 6. Mandible fragment of *Kubanochoerus* sp., CEESV0028, in occlusal view (A) and in left view (B). Scale bar = 5 cm.

Fig. 7. Occlusal view of cheek teeth of *Turcocerus* cf. *kekemaidengensis*. (A) Right cheek teeth row, CEESV0001. (B) Left P4 to M2, CEESV0003. (C) Right M3, CEESV0009. (D) Right p2, CEESV0021. (E) Right p3, CEESV0022. (F) Left m2 to m3, CEESV0016. (G) Right p4 to m2, CEESV0014. Scale bar = 2 cm.

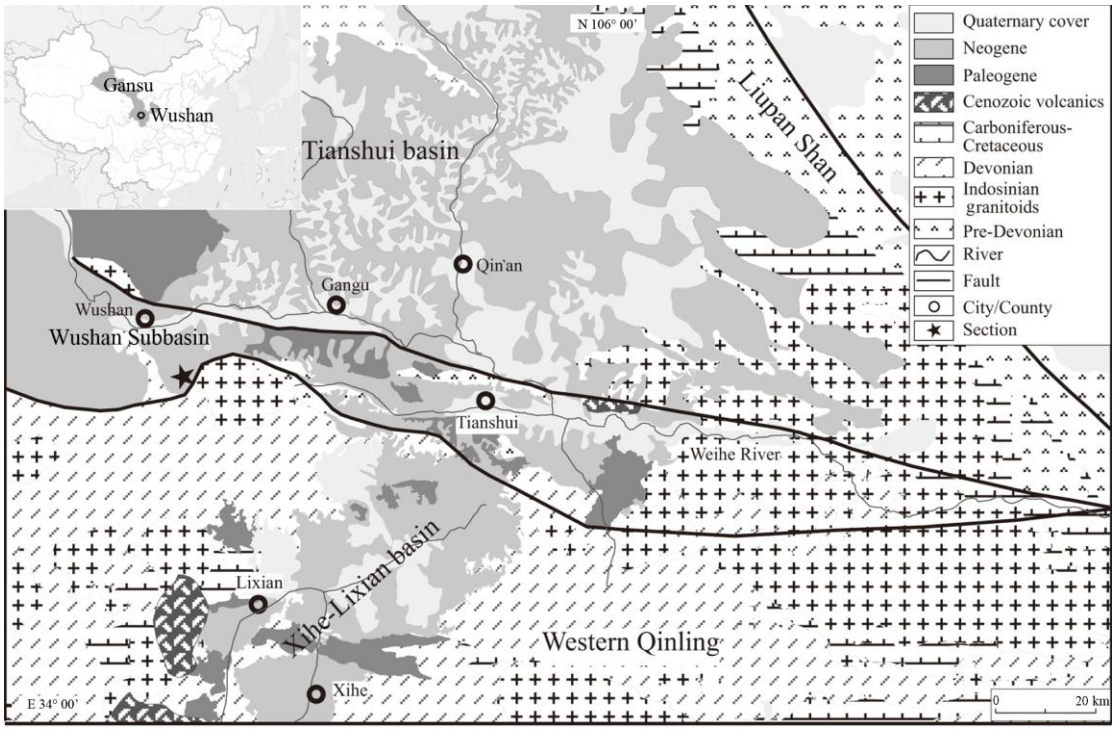

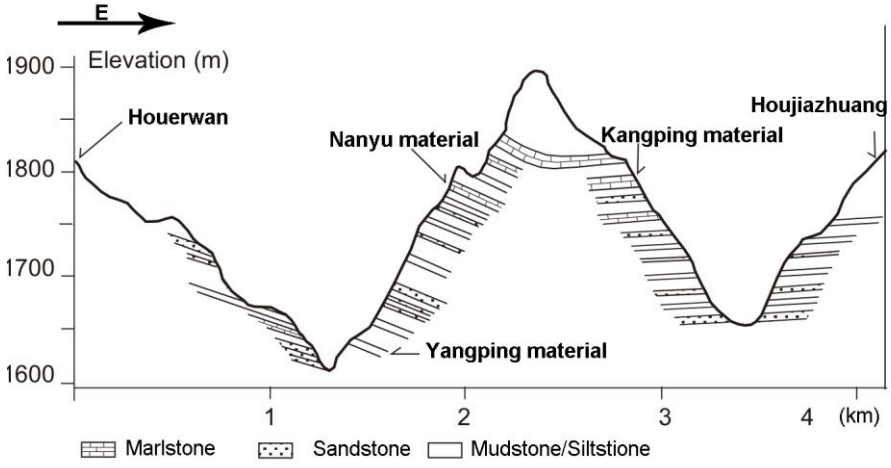

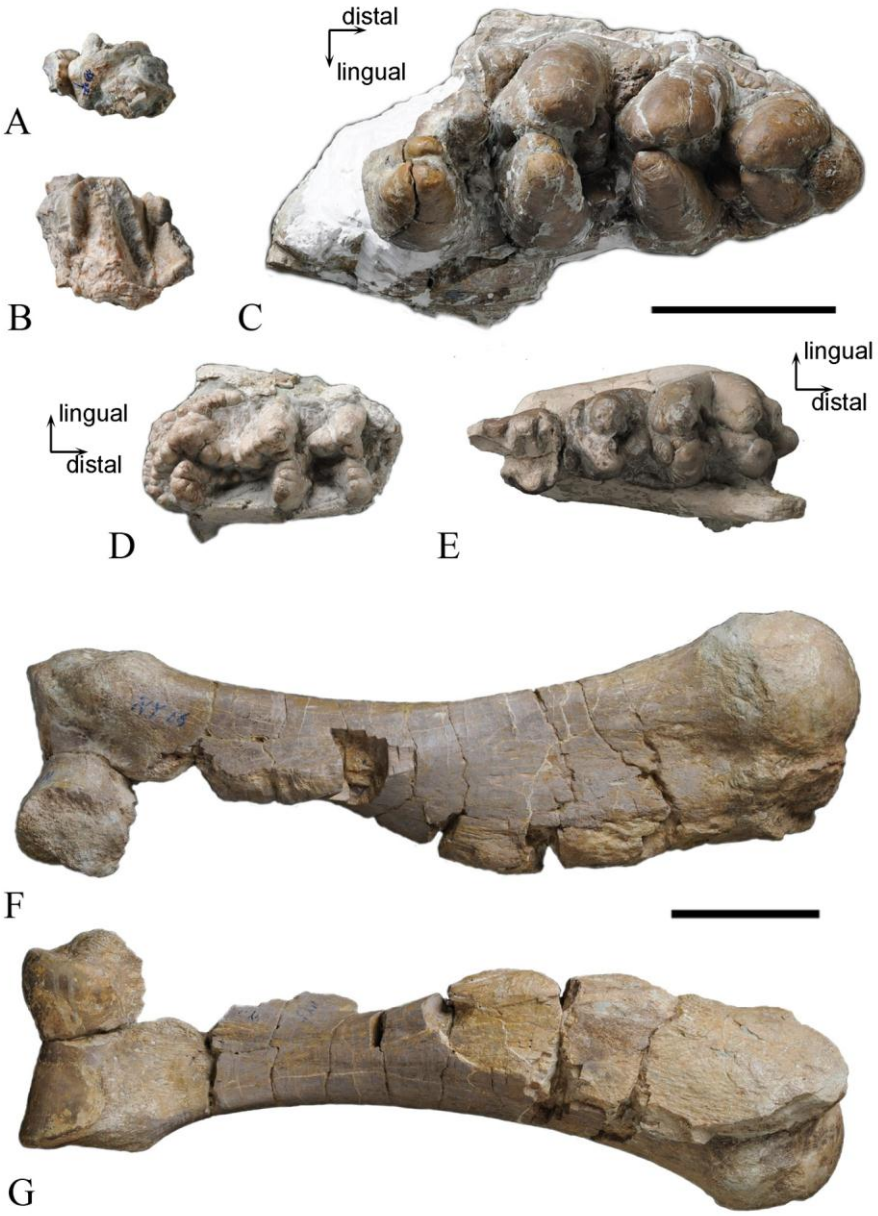

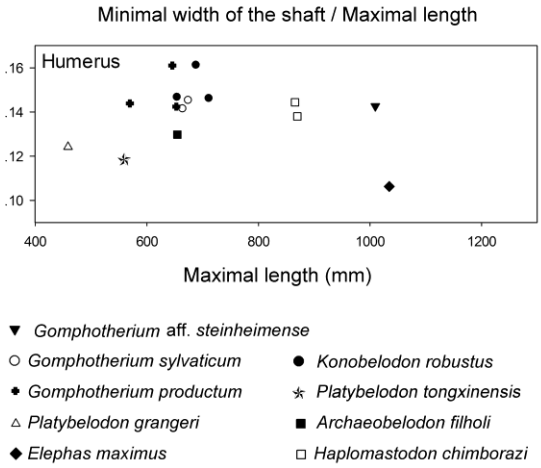

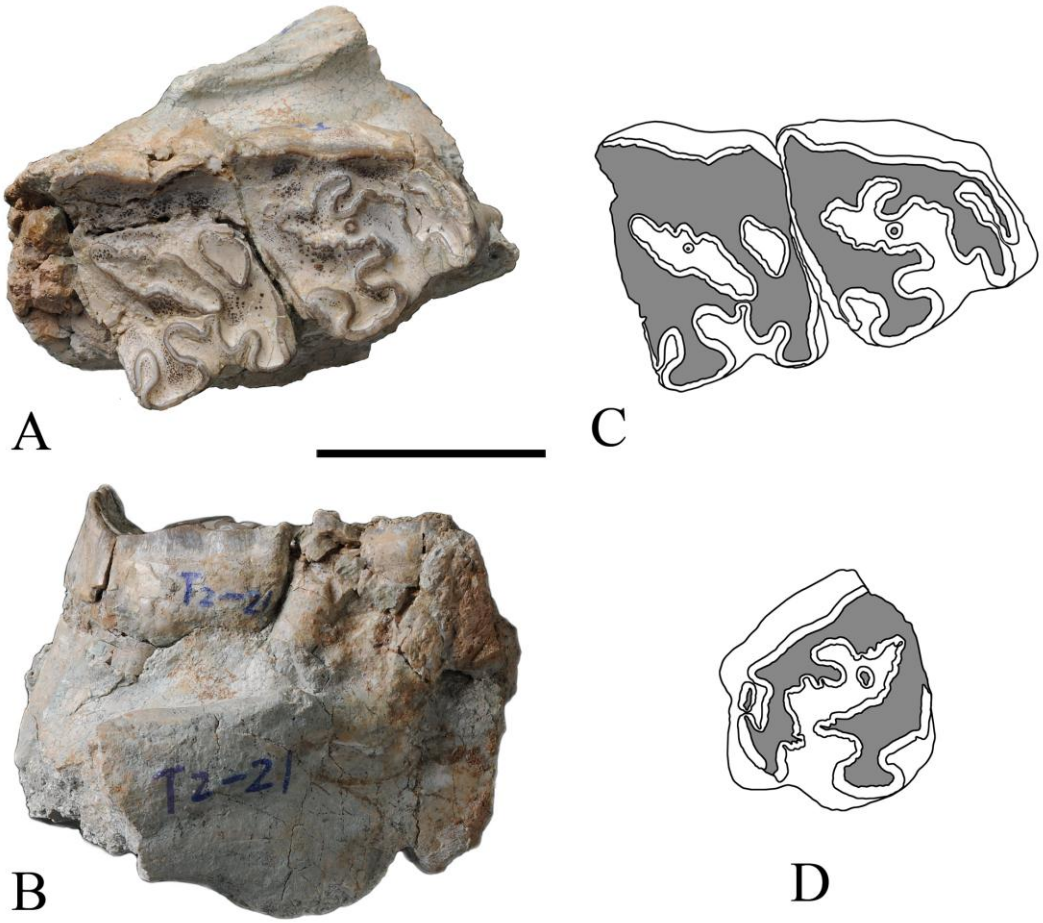

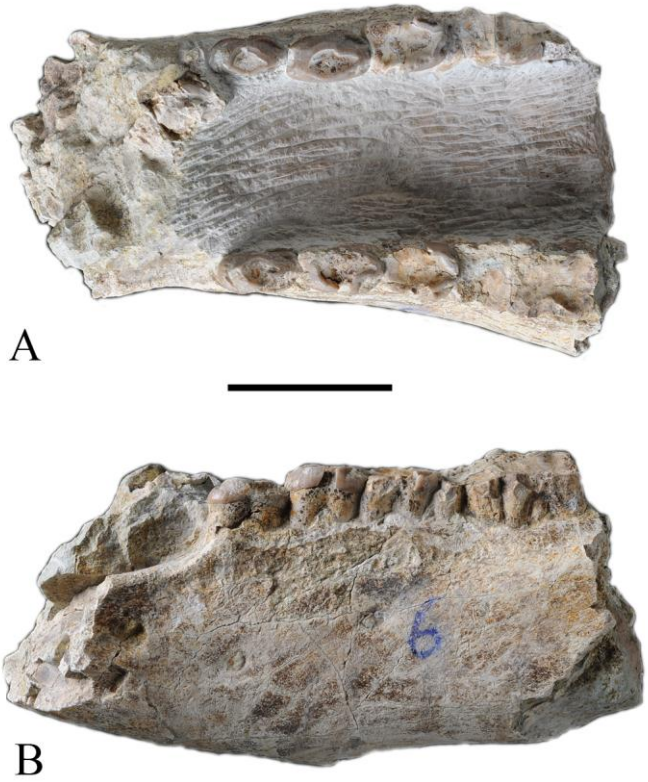

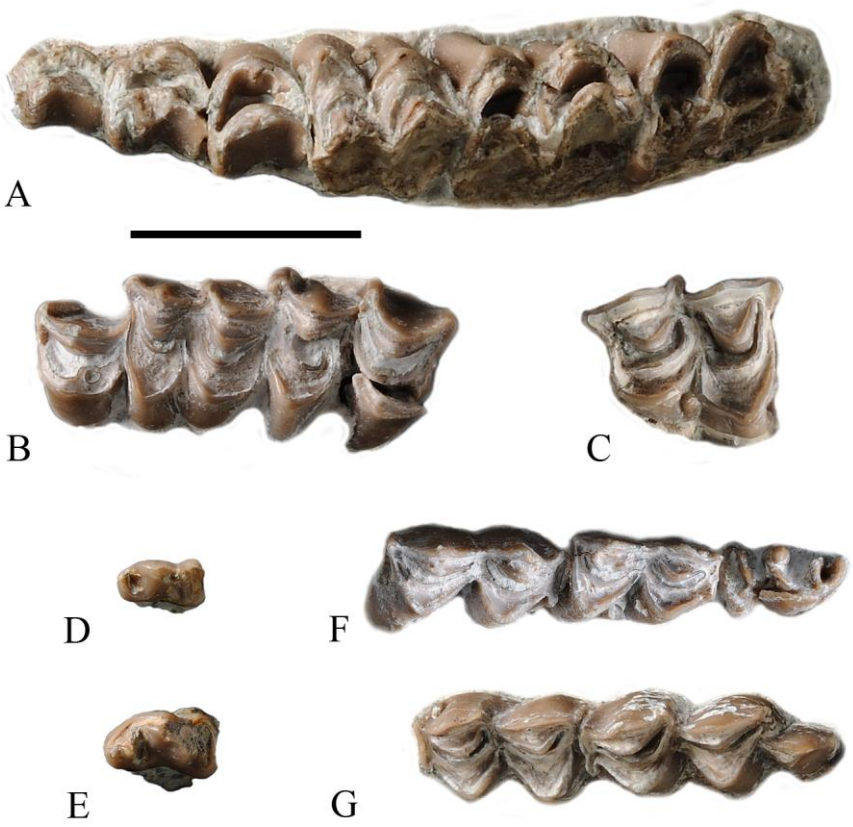

Table 1. Measurements of humerus of Proboscidae.

	Konobelodon robustus	*Gomphotherium sylvaticum*	*Gomphotherium* aff. *steinheimense*	*Platybelodon grangeri*	*Platybelodon tongxinensis*	*Haplomastodon chimborazi*	*Archaeobelodon filholi*	*Elphas maximus*
ML	655−712	665−675	1010	459	> 559.6	866−870	655	1035
MW/ML	0.1460−0.1611	0.1414−0.1452	0.1426	0.1242	< 0.1185	0.1379−0.1443	0.1298	0.1063

ML: maximal length (mm); MW/ML: ratio of minimal width of the shaft to maximal length.

Table 2. Measurements of M2 and M3 of *Hispanotherium* (in mm).

Teeth		*H. materitense*		*H. tunggurense*	*H. wushanense* n. sp.
		Laogou	Spain		
M2	L	49.9−56.0	51.9−52.1	60.9−64.6	41.0
	W	55.0−57.0	57.5−59.4	63.5−73.1	57.6
M3	L	47.0−45.9	56.0−57.7	46.4−60	45.8
	W	49.5−50.5	37.5−41.8	56.6−67.5	51.9

Data of the Laogou material are after Deng (2003); data of the Spain material are after Sanisidro et al. (2012); data of *H. tunggurense* are after Cerdeño (1996); L, length; W, width.

Table 3. Measurements of lower cheek teeth of bunodont listriodont suids in China (in mm).

Teeth		Wushan material	*Kubanochoerus minheensis*	*Kubanochoerus lantanensis*	*Kubanochoerus robustus*	*Bunolistriodon intermedius*
p2	L	22.3−24.8	27.0−28.0	30.0−33.0	34.1	
	W	12.3−12.8	13.5−14.8	14.7−15.0	16.6	
p3	L	24.3−25.0	26.5−27.4	34.0	34.9	17.0
	W	14.8−15.3	15.1−15.4	19.0	20.0	10.1
p4	L	23.0−4.0	26.0−27.4	30.5−30.6	34.5	17.0
	W	17.6−17.7	18.4−19.0	21.2−21.6	22.0	12.1−12.2
m1	L	16.5−16.9	27.1	29.0−34.6	34.5	20.3
	W	24.6	21	22.9−24	24.6	13.4
m2	L	26.2	31.3	38−38.2	39.3	21.9−23.4
	W	25.4	21.4	28.2−29	29	17.0−18.0

Data of *Kubanochoerus* are after Qiu et al. (1988); data of *Bunolistriodon* are after Ye et al. (1992); L, length; W, width.

Table 4. Measurements of cheek teeth of *Turcocerus* in China (in mm).

Measurement	*T. jiulongkouensis*	*T. robustus*	*T. stenocephalus*	*T. grangeri*	*T. noverca*		*T. kekemaidengensis*	
					Xining	Tunggur	Wushan	Duolebulejin
Length of upper cheek tooth row	72.6−74.1	74.3−81.9	73	88−91		63	66.9	
Length of upper premolar row	27.3−28.1	27.5−33.4	26	33		24	26.6	
Length of M3	17.9−19.5	20−22	18.8	19	11.3		15.9−18.3	
Width of M3	12.2−15.5	15.5−17.4	16.8	18	10.7		13.6−14.1	
Length of lower cheek tooth row	78.4−85.2							68.7
Length of lower premolar row	23.8−28.3							24.7
Length of m3	22.4−23.3						15.5−22.2	18.2−21.4
Width of m3	8.2−9.6						6−8.9	8−8.7

Data source: *T. jiulongkouensis*, *T. robustus*, *T.stenocephalus*, *T. grangeri*, *T. noverca* in Tunggur, after Chen and Wu (1976); *T. noverca* in Xining basin, after Qiu et al. (1981).